一般社団法人　電子情報通信学会
THE INSTITUTE OF ELECTRONICS,
INFORMATION AND COMMUNICATION ENGINEERS

信学技報
IEICE Technical Report
A・P2023-68(2023-08)

Design and Experimental Study on 1-Bit Time-Modulated Reflectarray

Xianbo CAO †, and Qiang CHEN †

† Department of Communications Engineering, Graduate School of Engineering, Tohoku University
6-6-05, Aramaki Aza Aoba Aoba-ku, Sendai, Miyagi 980-8579, Japan

E-mail: † cao.xianbo.s7@dc.tohoku.ac.jp, qiang.chen.a5@tohoku.ac.jp

Abstract In this report, a 1-bit time-modulated reflectarray (1-bit TMRA) is proposed and experimentally studied. By analyzing the intrinsic similarities between the reflection states of 1-bit reconfigurable reflectarray (1-bit RRA) and the logic states of 1-bit phase modulation time function, the 1-bit TMRA is devised by combining a conventional 1-bit RRA with time modulation (TM) technology. The operating principle and hardware design process are demonstrated in detail. A 10×10 prototype is fabricated and experimentally verified. The results show that the proposed 1-bit TMRA can achieve amplitude control at the carrier frequency. This advantage highlights the potential of the proposed 1-bit TMRA for practical applications in reconfigurable intelligent surfaces (RISs).

Key words Reflectarray, Time-modulated reflectarray, Reconfigurable intelligent surface

1. Introduction

Awareness of the pending resource depletion crisis has led to the proposal and vigorous development of renewable energy technologies. Researchers have proposed the concept of resilient electric power and information communication technology (R-EICT) to achieve autonomous decentralized cooperative control of power and communications to improve energy efficiency and the disaster resilience of the power and communication system [1][2]. However, the signal fading caused by electromagnetic scattering by buildings and other shielding has made it challenging to connect container-type data centers to high-speed, broadband, low-latency 5G/beyond 5G radio access networks (RANs). The reconfigurable intelligent surface (RIS) was introduced to address this issue.

Most hardware implementations of RISs are reconfigurable reflectarrays (RRAs). Among them, the real-time beam control achieved by the 1-bit RRA makes it suitable for RIS applications. The element of the 1-bit RRA is connected to an electronically controlled device, and the state of the electronically controlled device can be controlled to obtain two reflection phases with 180° (1-bit) difference. By selecting the 1-bit phase state of each element of the array to form a specific phase distribution, the direction of the reflected beam is controlled [3]-[5]. While the 1-bit RRA allows flexibility in controlling the beam direction, it does not provide control of the reflected amplitude. As such, it does not meet the final requirement of beamforming for RIS applications.

Recently, time-modulated reflectarrays (TMRAs) are attracting attention because they allow the flexible control of both amplitude and phase distribution. The basic concept of TMRAs is to modulate the RRA in a periodic manner by switching the RF switches on and off to control the scattering status of the RRA elements in a pre-designed time sequence [6]. However, most existing TMRAs work at harmonic frequencies, which has drawbacks of low efficiency and practicability.

In this report, we first clarify the intrinsic connection between 1-bit RRA and time sequence in TM technology and propose a novel 1-bit TMRA. Compared with 1-bit RRA, the proposed 1-bit TMRA has a capacity of amplitude control; compared with traditional TMRA, it works at the carrier frequency and has additional ability of phase control (omitted in this report due to page limit). These advantages make 1-bit TMRA versatile to meet requirements of different communication scenarios and more practical.

2. 1-bit TMRA Concept and Description

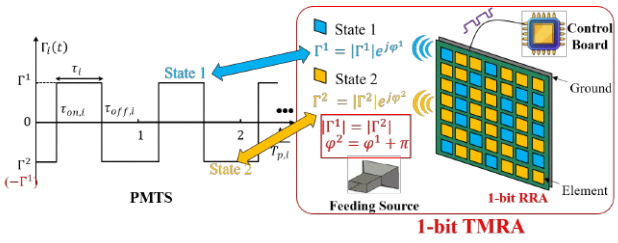

Fig. 1. Concept of 1-bit TMRA.

Previous studied of TMRA used strong/weak reflection states of RRA to realize high/low logic states of time sequence, which makes them inefficient and impractical in the actual applications. Thus, we considered the possibility of using two strong reflection states to achieve TMRA. Interestingly, the 1-bit RRA has two strong reflection state with the same amplitudes and opposite phases. Therefore, it is natural to use these two strong reflection states to correspond the two logic states of time sequence. We named this concept that uses a 1-bit RRA to realize TMRA as "1-bit TMRA". Since the two logical states have same amplitudes but opposite phases, this kind of time sequence is called phase modulation time sequence (PMTS). The corresponding relationship between 1-bit TMRA and PMTS is shown in Fig. 1.

The corresponding Fourier coefficients of PMTS, which are the equivalent reflection coefficients of each element, can be mathematically expressed as follows:

$$a_{i,h}(t) = \frac{1}{T_{p,i}} \int_0^{T_{p,i}} \Gamma_i(t) e^{-j2\pi h F_{p,i} t} = \begin{cases} 2\tau_i \operatorname{sinc}(\pi h \tau_i) e^{-j\pi h(\tau_{off,i}+\tau_{on,i})}, & h \neq 0 \\ 2\tau_i - 1, & h = 0 \end{cases}$$

It can be found that TM introduces an amplitude control ability at the carrier frequency, and the equivalent amplitude excitation is determined by duration time.

3. Design of 1-bit TMRA and Control Board

The configuration of the proposed 1-bit TMRA element is shown in Fig. 2(a). The polarization of the electric field is along the *x*-axis. The microstrip patch as a scatterer is printed on the top side of the element and connected to one end of the phase delay line printed on the bottom side through the metallization vias. A PIN diode is placed in the middle of the phase delay line, and the resonant property of the element is changed by biasing the circuit to turn the diode ON or OFF the diode, thus obtaining a 180° phase difference.

The initial structure of the element is inspired by the work reported by Yang et. al [7]. To achieve a center operating frequency of 10 GHz, the periodicity of the element *p* is set at 10 mm to avoid grating lobes. The main geometrical parameters of the 1-bit TMRA element are as follows: $lx = 7$ mm, $ly = 6$ mm. The thicknesses of the three substrate layers from top to bottom are 1.5 mm, 0.1 mm, and 0.5 mm, respectively. Since it offers low insertion loss and ultra-high switching speed, MACOM MA4AGFCP910 is chosen as the PIN diode, which acts as a switch in TM. For ON or OFF state, the PIN diode is modeled as a series of lumped resistance (R) and inductance (L) or capacitance (C) and inductance (L), respectively [8]. Fig. 2(b) shows the simulated reflection amplitude and phase difference using Floquet ports and periodic boundaries in HFSS. At 10 GHz, the 180° phase difference is obtained when the PIN diode turns from one state to another. From 9.72 GHz-11.03 GHz, the phase difference between the two states is within 180°±20°, indicating good element-bandwidth performance. The element loss is less than 0.6 dB within the frequency band of interest,

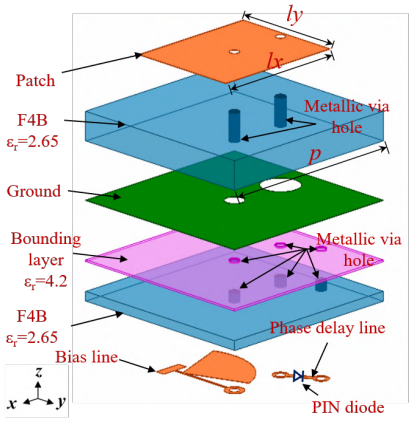

(a)

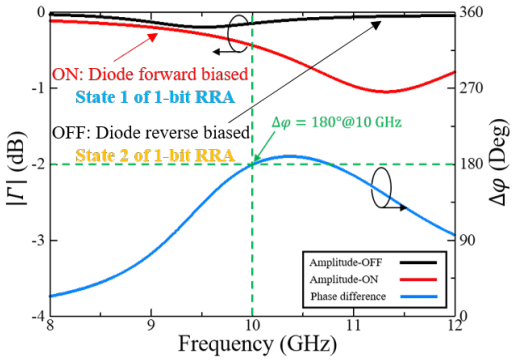

(b)

Fig. 2. 1-bit TMRA element. (a) Perspective view. (b) Simulated reflection amplitude and phase difference for the two states.

regardless of the PIN states.

Based on the proposed element structure, we designed and fabricated a 1-bit TMRA prototype using printed circuit board (PCB) technology, as shown in Fig. 3. The 1-bit TMRA has an aperture of 100 mm × 100 mm. Each element is soldered with a PIN diode and connected to a specific bias line to achieve 100 elements independently controllably. The TMRA and the control board are soldered with sockets, which are connected to each other by flat cables.

As shown in Fig. 4(b), control board for TM function was designed and fabricated. One column of the TMRA is set up as a group for control: this column has ten elements and is constrained by the quantity of the function generator. As shown in Fig. 4(a), the Chebyshev

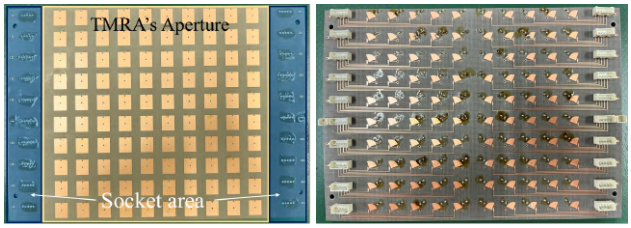

(a) (b)

Fig. 3. Photos of fabricated 10×10 1-bit TMRA prototype. (a) Front view. (b) Back view.

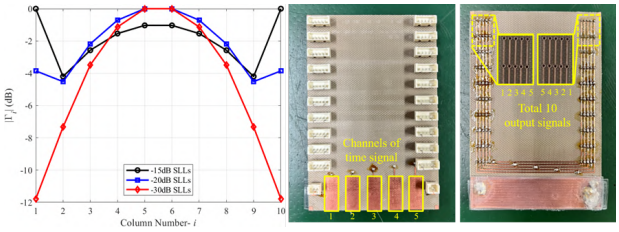

(a) (b)

Fig. 4. Control board design. (a) Desired |Γ| distribution. (b) Photo of fabricated control board.

distribution is symmetric about the center of the TMRA. This allows 10 groups (100 elements) to be controlled using 5-channel time signals (20 elements per channel).

4. Experimental Validation and Results

Fig. 5 shows the experimental environment and measurement system to verify the TM function. The measurement system consists of the 1-bit TMRA system, the rotary table, and the receiving antenna (Rx). The 1-bit TMRA system includes the 1-bit TMRA, the control board and the transmitting antenna (Tx). The control board is placed at the back of the TMRA and connected to the TMRA using the flat cables (not marked in Fig. 4). The relative position of the TMRA and Tx is kept constant in the rotation of the rotary table. The Tx and Rx are fixed in the far-field region of the TMRA, and the angle between its central axis and the normal of the TMRA aperture is defined as the scanning angle θ. Therefore, by rotating the rotary table in the horizontal plane, the radiation pattern of the 1-bit TMRA can be measured. Note that the operating frequency in the following experiments is set as

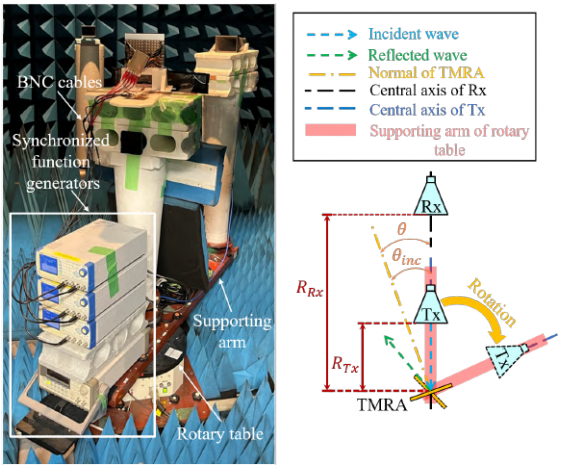

(a) (b)

Fig.5. Experimental environment for validation of time modulation characteristics. (a) Overall perspective photo. (b) Schematic diagram of the measurement system.

11.1 GHz.

Note that the normalized scattering pattern is measured with this experimental environment to properly evaluate the scattering performance of the proposed 1-bit TMRA. The experimental target is to realize the scattering pattern with -20 dB equal SLLs by means of TM. The modulation frequency is 100 kHz. Fig. 6(a) shows the required time sequence of each channel. The dark area corresponds to the state "1", which corresponds to the diode ON state, and the light square corresponds to the state "-1", which corresponds to the diode OFF state.

The measured results are shown in Fig. 6(b). Note that the results of the metal sheet are plotted as a benchmark. It can be first observed that among the three results, the first side-lobe level (SLL) on the left side of the main beam is larger than the first SLL on the right side by nearly 2 dB in all cases. This reflects the oblique reflection characteristic under this environment. It is found that the SLLs are significantly reduced by TM. Specifically, except for the first SLL (2° direction) on the left side of the main beam, the other three SLLs near the main beam are -22.53 dB (-7.5° direction), -19.74 dB (38.5° direction), and -19.74 dB (54.5° direction) respectively. That is, the

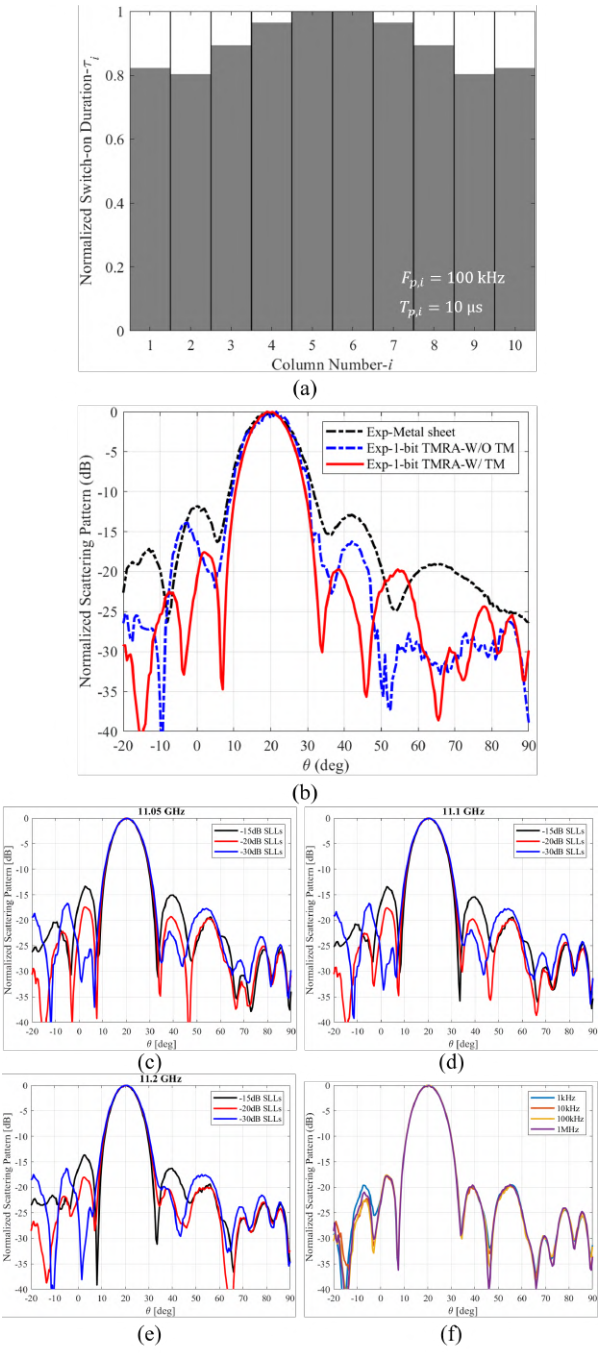

Fig. 6. Experimental results. (a) Switch-on duration τ_i. (b) Measured normalized scattering patterns. Detailed photo of TMRA placement. (c) Schematic diagram of the measurement system. (d)-(e) Scattering patterns for different frequencies and targets. (f) Scattering pattern of different modulation frequencies.

experimental target is basically achieved. The imperfection can be attributed to the relatively small size of the fabricated 1-bit TMRA, which also leads to the uncontrollability for the SLLs within a large-angle range.

It is worth mentioning that the maximum scattering strength of the result of TM is only 1.6 dB smaller than the results of the metal sheet, which indicates good efficiency of the 1-bit TMRA. The loss is mainly caused by the losses of the diodes and harmonic frequencies. In summary, the TM function of the proposed 1-bit TMRA is verified by the experiment.

To further evaluate the performance of the TM, the normalized scattering patterns for different frequencies of realizing equal SLLs of -15 dB and -30 dB are measured and plotted together with the results of form equal -20 dB SLLs in Fig. 6(d). As can be seen from the figure, the measured main beams are the same for the different time sequences, while the sidelobes are different, which indicates that the TM achieves effective control of the SLLs. Also, the equal -15 dB and -20 dB SLLs are clearly successfully achieved. The results of forming -30 dB SLLs indicate that only the reduction of the first SLL is achieved, while the other SLLs are not effectively controlled. The main reason for this is that the small aperture in the fabricated prototype results in a weak reflection, which makes it difficult to achieve ultra-low SLLs.

Besides, the measured results of 11.05 GHz and 11.2 GHz are also plotted in Fig. 6(c) and (e). The good agreement of the results for different frequencies is evidence of frequency stability in the time-modulated scattering pattern. It should be noted that the maximum scattering strength of the main beam does not fluctuate more than 1 dB over the entire measurement band (10.75 GHz-11.2 GHz). Note that we define an SLL bandwidth as the frequency range in which the difference between the first right SLL and the design target (-20 dB in this experiment) does not exceed 1dB. The measured results show that the SLL bandwidth exceeds 250 MHz. However, from the signal transmission point of view, it is necessary for the bandwidth of the time-modulated signal to be smaller than the TM frequency F_p (100kHz in this work) to avoid spectrum aliasing [9]. That is, the operating bandwidth of the proposed 1-bit TMRA system is mainly limited by the TM frequency.

The normalized scattering patterns for different TM frequencies are also measured and are plotted in Fig. 6(f). From 1 kHz to 1 MHz, the measured results remain essentially the same, which verifies that the modulation frequency does not affect the scattering characteristic of the TMRA. Note that in this experiment, the upper limit of the modulation frequency is determined by the function generator. In most case, the modulation frequency is determined by the operating frequency of the switching components (e.g., diodes, MEMS, etc.) and the operating frequency of the time signal generated by the control board.

5. Conclusion

In this investigation, we successfully designed a 1-bit 10×10 TMRA for RIS applications at the X-band and then verified it experimentally. We identified the intrinsic similarities between the reflection states and logic states of time function, and designed the proposed the 1-bit TMRA based on our findings. The proposed 1-bit TMRA has the characteristics of the conventional 1-bit RRA and can shape radiation patterns through TM at the center operating frequency to cope with different communication scenarios.

The TM function is verified by shaping the scattering pattern with ultra-low SLLs. It is shown that the proposed 1-bit TMRA can achieve a scattering pattern with equal -20 dB SLLs, with a maximum scattering strength only 1.6 dB less than that of the same size metal sheet. This small reduction of the scattering strength indicates well efficiency of the proposed 1-bit TMRA.

It is shown that it is not the radiation characteristic bandwidth (gain and SLL bandwidth) but the TM bandwidth which is the key factor limiting the bandwidth of 1-bit TMRA operation. The experiment also validated

that the modulation frequency does not affect the radiation characteristics of 1-bit TMRA.

The findings of this study can be used as a resource for refining the theory of TM technique-based RRA design. The proposed 1-bit TMRA has practical potential in RIS applications, and further developments will contribute to the beyond 5G and 6G technologies of the future.

6. Acknowledgement

This work was supported in part by the Program on Open Innovation Platform with Enterprises, Research Institute and Academia, Japan Science and Technology Agency (JST, OPERA, JPMJOP1852).

7. References

[1] T. Otsuji, K. Iwatsuki, H. Yamada and M. Yashima, “Concept of Resilient Electric Power and Information Communication Technology (R-EICT) Converged Network Systems Based on Overall Optimization of Autonomous Decentralized Cooperative Control of DC Microgrids,” 2021 IEEE Power & Energy Society Innovative Smart Grid Technologies Conference (ISGT), 2021, pp. 1-5.

[2] Toru Tanaka, Hiroya Minami, et al. “Energy-distribution Platform Technologies toward Zero Environmental Impact” NTT Technical Review. Vol. 19 No. 6 June 2021.

[3] M. A. ElMossallamy, H. Zhang, L. Song, K. G. Seddik, Z. Han and G. Y. Li, "Reconfigurable Intelligent Surfaces for Wireless Communications: Principles, Challenges, and Opportunities," IEEE Transactions on Cognitive Communications and Networking, vol. 6, no. 3, pp. 990-1002, Sept. 2020.

[4] Z. Wang et al., "1 Bit Electronically Reconfigurable Folded Reflectarray Antenna Based on p-i-n Diodes for Wide-Angle Beam-Scanning Applications," IEEE Trans. Antennas Propag., vol. 68, no. 9, pp. 6806-6810, Sept. 2020.

[5] H. Xu, S. Xu, F. Yang and M. Li, "Design and Experiment of a Dual-Band 1 Bit Reconfigurable Reflectarray Antenna With Independent Large-Angle Beam Scanning Capability," IEEE Antennas Wireless Propag. Lett., vol. 19, no. 11, pp. 1896-1900, Nov. 2020.

[6] Y. Wang and A. Tennant, "Experimental Time-Modulated Reflector Array," IEEE Trans. Antennas Propag., vol. 62, no. 12, pp. 6533-6536, Dec. 2014.

[7] H. Yang et al., "A 1-Bit 10×10 Reconfigurable Reflectarray Antenna: Design, Optimization, and Experiment," IEEE Trans. Antennas Propag., vol. 64, no. 6, pp. 2246-2254, June 2016.

[8] Cao X, Chen Q, “Design of Multifunctional Reflectarray Elements Based on the Switchable Ground Plane” Int. Symp. Antennas Propag.(ISAP)., 2021, pp.1-2.

[9] J. C. Bregains, J. Fondevila-Gomez, G. Franceschetti and F. Ares, "Signal Radiation and Power Losses of Time-Modulated Arrays," IEEE Trans. Antennas Propag., vol. 56, no. 6, pp. 1799-1804, June 2008.